



Noble metal and graphite formation in metamorphic rocks of the Khanka terrane, Far East Russia



A.I. Khanchuk^{a,b,*}, L.P. Plyusnina^a, N.V. Berdnikov^c

^a Far East Geological Institute of the Russian Academy of Sciences, Prospekt 100-letia, 159, Vladivostok 690022, Russia

^b Far Eastern Federal University, Suhanova St., 8, Vladivostok 690950, Russia

^c Institute of Tectonics and Geophysics of the Russian Academy of Sciences, Kim U Chen Street, 65, Khabarovsk 680000, Russia

ARTICLE INFO

Article history:

Received 5 June 2014

Received in revised form 24 November 2014

Accepted 8 December 2014

Available online 24 December 2014

Keywords:

Noble metals

Carbon

Graphite

Metamorphism

Fluids

ABSTRACT

Noble metal–graphite mineralization has been identified in the Riphean–Cambrian metamorphic complexes of the northern Khanka terrane, Russia. The graphite mineralization is hosted in magmatic and sedimentary rocks metamorphosed under greenschist to granulite facies conditions. This paper provides the results of our study of the Turgenevo–Tamga graphite deposits. This study analyzes the geochemistry of the noble metals with the aim of determining the spatial relationships between noble metals and graphite. The graphitized rocks, analyzed by various geochemical methods, show a wide range of noble metal concentrations (ppm): Pt (0.02–62.13), Au (0.02–26), Ag (0.56–4.41), Pd (0.003–5.67), Ru (0.007–0.2), Rh (0.001–0.74), Ir (0.002–0.55), and Os (0.011–0.09). Crystallization from gas–condensates is indicated by the relationships between the noble metal mineralization and the graphite, and in particular the inhomogeneous distribution of graphite in the rocks, the inhomogeneous distribution of metals in the graphite, the microglobular graphite structures, and the carbon isotopic compositions. Thermal analysis and Raman spectroscopy indicate that some of the graphite formed from the metamorphism of sedimentary biogenic carbonaceous matter. The uneven distribution of noble metals in the rocks, and the compositional variability of the mineralization, implies that the origin of the metals was largely related to endogenic processes involving reduced fluids derived from depth. Our conclusion is that the noble metals and graphite mainly originated from magmatic fluids, but that some material was derived from exogenic and metamorphic sources.

© 2015 Elsevier Ltd. All rights reserved.

1. Introduction

The importance of fluid transport for the crystallization of metamorphic minerals has been recognized for many years (Korzhinskii, 1965; Ferry, 1996). The degree of volatile transport in carbonaceous complexes has been debated for many years, and it remains a problematic issue (Ferry, 1996; Manning, 2004; Galvez et al., 2013). Carbonaceous meta–terigenous sequences may contain economic deposits of gold, as for example in the large gold deposits of Muruntau in central Uzbekistan, Bakurchik, eastern Kazakhstan, Kumtor, Kyrgyzstan, Sukhoi Log, and the Patom Highlands, Russia (Yermolaev, 1995). These stratiform deposits consist of black shales that contain amorphous carbonaceous

matter of organic origin, but the possible enrichment of the rocks with endogenic carbon has been actively discussed (Vinokurov et al., 1997; Laverov et al., 2000). Fluid-driven deposition of graphite from cooling C–O–H fluids that permeated the lithosphere (along fractures) has been reported from the Stillwater complex, South Africa, the Borrowdale graphite deposit in the United Kingdom (Ortega et al., 2010), and the New Hampshire graphite deposits (Rumble et al., 1986). The ability of reduced carbon-bearing fluids from deep endogenic sources to accumulate and transfer metals is well established, and noble metal mineralization is well known in carbon-bearing sedimentary and magmatic rocks metamorphosed under the amphibolite and greenschist facies (Volborth and Housley, 1984; Ballhaus and Stampfl, 1985; Melcher et al., 1997; Distler et al., 2004; Wright et al., 2010). However, the nature of the fluid–rock interactions, as well as the mechanisms of graphite formation under relatively low-temperature conditions (especially $T < 500$ °C), remain unknown (Chamberlain, 1967).

* Corresponding author at: Far East Geological Institute of the Russian Academy of Sciences, Prospekt 100-letia, 159, Vladivostok 690022, Russia. Tel.: +7 9150423457.

E-mail addresses: axanchuk@mail.ru (A.I. Khanchuk), makarovo38@mail.ru (L.P. Plyusnina), nick@itig.as.khb.ru (N.V. Berdnikov).

Carbon is considered to play a significant role in ore-forming processes, particularly during the transport of noble metals in C–O–H–Cl ± F ± S-fluids (Ballhaus and Stampfl, 1985; Mogessie et al., 1991; Boudreau and McCallum, 1992). The participation of endogenic carbon during ore formation has been supported by the discovery of a new type of noble-metal mineralization in the Riphean–Cambrian metamorphic complexes of the northern Khanka terrane of Russian Primorye (Khanchuk et al., 2004, 2010). The graphitization here is of regional extent and affects rocks that have undergone greenschist to granulite-facies metamorphism, including schists, gneisses, granite gneisses, marbles, phyllites, and lamprophyre dikes. The graphitization is quite unlike the mineralization found in typical stratiform black-shales. In the Khanka terrane, exploration for graphite took place prior to 1950, particularly in the large deposits at Tamga (400 km²) and Turgenevo (225 km²) in the Lesozavodsk district of Primorye. Previous studies of these two deposits indicate a close association between the noble metal mineralization and the graphite. The aim of this study is to analyze the geochemistry of the noble metals, to determine the spatial relationships between noble metals and graphite, and to determine the sources of the carbon and the noble metals.

2. Geological setting

The graphite deposits of Turgenevo–Tamga are situated within the Khanka terrane, which is considered to be a Caledonian tectonic unit in the eastern continuation of the Central Asian Orogenic Belt. In the late Precambrian (730 Ma, according to the Sm–Nd method), the terrane underwent amphibolite and epidote–amphibolite facies regional metamorphism, and later, at the Cambrian–Ordovician boundary, greenschist to granulite facies metamorphism (Khanchuk et al., 2013). The granulites and amphibolites occur in the cores of narrow, tightly compressed folds, the axes of which mainly trend E–W, but with a few trending NW–SE and NE–SW. These rocks are cut by numerous faults of varying strike, and they are enveloped by a dome-like structure. Gabbroic and granitic intrusions of middle Paleozoic–Mesozoic age encircle the dome structure and occupy its center, whereas early Paleozoic granites seem to be distributed independently of the structure (Fig. 1).

The Turgenevo graphite deposit is situated in the Ruzhino metamorphic dome which contains amphibolite facies rocks of the Ussuri Group in its core. The complex is composed of garnet–biotite–feldspar and biotite–quartz–feldspar schists that are intercalated with marbles and conformable injections of biotite-rich and leucocratic granite gneiss. The schists are composed mainly of mafic minerals with a predominance (up to 40%) of biotite. Lens-shaped marble bodies, 10–75 m thick, were metamorphosed to skarns along the contacts with the granite gneiss, and they consist of calcite, zoisite, diopside, plagioclase, and K-feldspar. From the contact outwards, the skarns pass into diopside–calcite rocks, and then into marble. Thin (up to 1 m) lamprophyre and amphibolite dikes, conformable to the foliation of the country-rock schists, are enriched in TiO₂ and K₂O, and contain 0.6–30% graphite. Greenschist-facies carbonaceous rocks of the Mitrofanovka Formation outcrop along the southern edge of the Ruzhino dome (Fig. 1). The rocks are similar in appearance to black shales, and contain fine-grained quartz (60–80%), sericite, and graphite (up to 12%), and some chlorite. Weakly metamorphosed phyllites and metasilstones of the Kabarga Formation overlie the Mitrofanovka rocks, and are cut by metadolerite dikes. The chemical compositions of selected graphite-bearing rocks are listed in Table 1.

The Tamga deposit is hosted by a carbonate-gneiss that includes graphite-gneiss with economic coarse-flaky graphite that is suitable for crucibles. Numerous lenses of skarn and graphitized marble are incorporated within the gneiss. The grade of metamorphic

alteration would suggest the rocks of the Tamga graphite deposit are related to the Ussuri Group.

3. Research methods

The determination of noble-metal concentrations in graphite-bearing rocks is problematic because graphite is inert to almost all chemicals. The quantitative physicochemical methods used in this study include atomic emission spectrometry (AES), inductively coupled plasma-mass spectrometry (ICP-MS), and atomic absorption spectrophotometry by thermoelectric atomization with prior extract concentration (AAS-TEA), all of which have been previously used by other workers to analyze noble metals in carbonaceous terrigenous rocks (Kucha, 1981; Mitkin et al., 2000). To determine the concentrations of Pt and Au in the graphite-bearing rocks from the Khanka terrane, we mostly used AAS-TEA with a sensitivity of 10^{−8} wt%. Chemical decomposition was performed as follows. The samples were successively dissolved in mixtures of concentrated acids in the proportions HF:HNO₃ = 2:1, → HCl:HNO₃ = 3:1, → HCl. Next, the insoluble graphite residue was filtered and dissolved in HClO₄, and both solutions were combined and converted into 2N HCl. Finally, noble metals were extracted with alkyraniline, and concentrations were determined by AAS-TEA on a Shimadzu AA-6800 spectrophotometer. The AAS-TEA method provides more reproducible results compared with other techniques, but is time consuming. The results obtained by AAS analysis for Au, Pt, and Pd concentrations in soluble silicate fractions and in the graphite residue are listed in Table 2.

Some of the graphite-bearing samples were analyzed after preliminary decomposition by fluoroxidation (Table 3). This method was first developed for black shales (Mitkin et al., 2000) and then adapted for the analysis of graphitized rocks (Mitkin et al., 2009). The technique involves the fluoridation of samples with BrF₃ and KBrF₄, and after this, the fluorides are converted into chlorides and then analyzed by AAS or AES. High Au and Pt contents were first discovered in the graphite-bearing rocks of the Khanka terrane by ion mass spectrometry (IMS) analyses in 2004 performed by scientists of the Institute of Microelectronics and High-Purity Compounds, Russian Academy of Sciences, Chernogolovka. This method of analysis has an advantage in that it allows the high-sensitive detection of elements and noble metals in solid samples, and it does not require the preliminary dissolution of samples in strongly oxidizing reactants. The IMS analyses were conducted using an Element 2 ICP mass spectrometer manufactured by Thermo Electron Corporation. The spectrometer was equipped with a glow-discharge ion source based on a hollow cathode installed instead of an ICP-source sampler (Sikharulidze, 2004, 2009). Application of a new source of ions allowed us to analyze solid, non-conducting powder samples, and the high sensitivity of the method made it possible to analyze the powdered carbonaceous rock samples without pre-concentration of the metals. In addition, IMS allows the imaging of spectra for a wide range of metals and their isotopes. In earlier methods of analysis, the dissolution of samples at high temperatures often led to a drop in the detected values of the metals due to the emission of some carbon–metallic volatile complexes; the IMS method avoids this problem. The value of the IMS method is supported by comparisons of analytical results produced by both the AAS and IMS methods for the same samples (Table 4). Carbon isotope measurements were made using a Finnigan MAT-252 mass spectrometer at the Analytical Center of the Far East Geological Institute of the Far Eastern Branch of the Russian Academy of Sciences (FEGI FEB RAS), Vladivostok, Russia. Carbon isotope compositions in the graphite-bearing rocks of the Ussuri and Mitrofanovka formations are listed in Table 5.

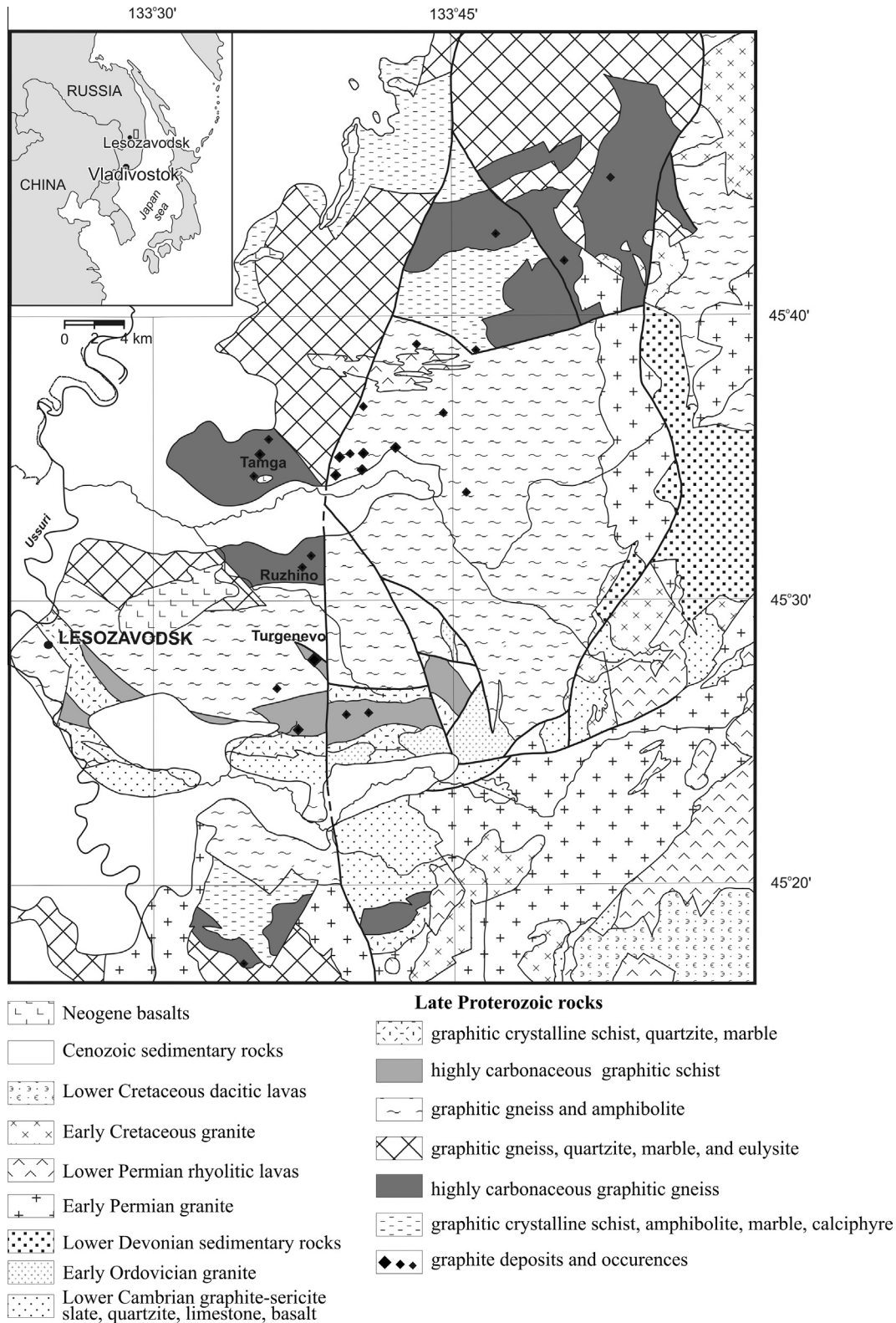


Fig. 1. Schematic geological map of the northern Khanka terrane.

The rock samples in polished sections, fresh rock chips, and separate grains were also studied with a scanning electron microscope EVO-50XVP equipped with an energy dispersive X-ray spectrometer INCA Energy-350 (SEM EDA analysis) at the Analytical Centre of FEGI FEB RAS. It is noteworthy that the identification of native metal phases in graphite-bearing rocks is a difficult task. In pol-

ished sections, the soft graphite spreads over the surface of the section, and minute hard grains of metal are crumbled out. For this reason we used fresh chips of rocks without polishing. In some cases the surface of a chip was etched with strong acids, which made it relatively easy to find microcrystals of native noble metals. Moreover, electron energy loss spectroscopy (EELS) was used to

Table 1

Chemical compositions (wt%) of rocks from the Tamga and Turgenevo graphite deposits in the Ussuri and Mitrofanovka formations (silicate method).

Sample	02/3	03/3	04/17	04/40	04/7a	04/30	04/101	02/1	02/4
SiO ₂	37.74	38.56	81.26	68.30	51.30	52.50	52.07	70.82	66.50
TiO ₂	0.19	0.32	0.42	0.75	1.16	1.18	1.04	0.22	0.05
Al ₂ O ₃	12.03	8.95	7.20	12.32	21.31	19.57	19.29	12.61	12.33
Fe ₂ O ₃	0.29	2.18	2.20	4.33	3.39	1.94	7.57	0.58	1.81
FeO	5.50	0.85	0.34	0.62	6.05	7.08	1.76	tr	tr
MnO	0.03	0.06	0.01	cπ	0.03	0.17	0.10	0.02	0.01
MgO	0.58	2.16	0.40	0.80	1.78	4.11	4.01	0.32	0.62
CaO	0.20	2.51	0.18	cπ	1.95	1.53	1.30	3.04	0.28
Na ₂ O	0.93	1.83	0.47	0.63	2.61	2.94	2.67	0.95	1.90
K ₂ O	3.03	1.58	2.20	3.31	6.75	6.77	7.31	7.90	6.38
P ₂ O ₅	tr	tr	0.12	0.23	0.12	0.32	0.29	tr	tr
H ₂ O ⁻	0.59	tr	0.22	0.10	0.21	tr	tr	0.10	tr
H ₂ O ⁺	3.73	5.97	2.11	3.69	2.59	1.58	1.47	0.98	2.45
C	36.47	34.57	3.24	4.52	0.33	0.60	0.77	2.08	7.33
Σ	101.31	99.54	100.37	99.60	99.58	100.29	99.65	99.62	99.66

Note: samples 02/3 and 03/3 are schists from the Ussuri Formation; 04/17 and 04/40 are graphite-sericite-quartz shales from the Mitrofanovka Formation; 04/7a, 04/30, and 04/101 are lamprophyres; and 02/1 and 02/4 are granite-gneisses. tr = trace amount.

Table 2

Noble metal contents (ppm) in selected rock samples from the Khanka terrane, as determined using soluble silicate fractions and graphite residues.

Sample	Au*	Graphite			ΣAu	C (wt%)	Rock
		Au	Pt	Pd			
02/1	0.73	16.68	8.68	5.67	17.41	35	Graphitic metasomatic rock
02/3	0.56	2.83	2.15	0.99	3.39	4.7	Plagiogneiss with graphite
02/4	0.61	4.18	2.39	1.23	4.79	6.3	Granite gneiss
03/1a	–	2.56	4.14	3.31	2.56	5.6	Graphitic metasomatic rock
03/3	0.1	5.37	14.15	7.31	5.47	30	Garnet-biotite-graphite schist
03/5	1.26	0.04	4.46	1.24	1.30	29	Lamprophyre

Note: Au* = gold in solution after the initial treatment of samples with aqua-regia; Au, Pt, and Pd were measured in the graphite residue after its decomposition in HF and HClO₄ (analyses were performed using AAS).

Table 3

Noble metal contents (ppm) in graphite-bearing rocks from the Tamga and Turgenevo graphite deposits, as determined after fluoroxidation of samples.

Sample	Au	Pt	Pd	Rh	Ru	Ir	Os	Ag	Rock
1a	0.021	0.039	0.047	0.005	–	–	–	0.893	Granite gneiss
	0.709	–	0.025	–	–	–	–	–	
2a	0.11	0.026	0.014	0.004	–	–	–	1.384	Amphibolite
	0.636	–	0.035	–	–	–	–	–	
13	0.025	0.025	–	–	–	–	–0.019	–	Amphibolite
	1.43	0.021	–	–	0.076	0.02	–	4.41	
16	0.27	0.116	0.274	0.003	–	–	–	–	Graphite-sericite-quartz shale
	1.892	0.02	0.16	0.011	–	0.004	0.011	0.502	
40	0.23	0.038	0.048	0.005	–	–	–	–	Lamprophyre
	6.73	0.011	0.042	–	0.012	0.006	0.013	0.15	
29	0.26	0.045	0.149	0.007	–	–	–	–	Lamprophyre
	1.61	0.020	0.096	–	0.045	0.019	0.029	0.024	
31	0.022	0.014	0.012	0.006	0.007	–	–	–	Skarn
	1.90	0.024	0.59	–	0.038	0.011	0.016	2.07	
34	0.23	0.057	0.92	0.46	–	–	–	–	Marble
	2.012	0.023	0.104	–	0.045	0.009	0.017	0.12	
34a	0.30	0.093	0.043	–	–	–	–	–	Marble
	2.23	0.020	0.090	–	0.035	0.015	0.017	0.27	
80	0.246	0.017	0.051	–	–	–	–	–	Skarn
	0.04	–	0.429	–	–	–	–	1.111	
107k	0.24	–	0.031	–	–	–	–	–	Marble
	0.076	0.036	0.223	–	–	–	–	3.46	
108	0.130	0.094	0.052	0.005	0.007	–	–	–	Graphite-quartz vein
	1.01	0.029	0.28	–	–	–	–	0.97	

Note: for the two values provided for each sample, the first (upper) value is the noble metal content in chloride solution after single rock fluoroxidation, and the second (lower) value is the noble metal content in the graphite insoluble residue in a sulfate solute. Analyses were performed using the atomic-emission spectroscopy method. Dashes in the table indicate 'not detected'. The total number of analyzed samples is 40, and the table shows the results for 12 selected samples.

detect platinum inclusions in graphite flakes from the Turgenevo deposit. The EELS allowed us to visualize the distribution of noble metals in any matrix on the nanometer scale (Leapman and Newbury, 1993).

The parameters of the graphite crystal lattice were studied with an XRD-6000 X-ray diffractometer (Cu anticathode). Additional data on the textural state of the carbonaceous matter were obtained using Raman spectroscopy with a high-resolution HR

Table 4

Gold and platinum contents (ppm) in rocks from the Turgenevo deposit, as determined by IMS and AAS (one analytical run).

Sample	Au	Pt	Method	Rock
02/3	13	4	IMS	Granite gneiss
	3.39	2.15	AAS	
03/1a	5	16	IMS	Granite gneiss
	2.56	4.14	AAS	
03/3	3	6.7	IMS	Garnet–biotite–graphite schist
	5.47	14.15	AAS	
03/5	5	52	IMS	Lamprophyre
	1.30	4.46	AAS	
04/7a	12	20	IMS	Skarn
	1.04	1.15	AAS	
04/7b	12	14	IMS	Skarn
	0.16	1.51	AAS	
04/17	7.2	5	IMS	Graphite–sericite–quartz shale
	0.66	1.30	AAS	
04/29	15	18	IMS	Lamprophyre
	0.46	1.28	AAS	
04/40	17	24	IMS	Graphite–sericite–quartz shale
	0.18	1.29	AAS	
04/9	2.2	3.3	IMS	Graphitic metasomatic rock
	0.14	0.82	AAS	

Table 5

Carbon isotopic compositions of rocks from the Ussuri and Mitrofanovka formations.

Sample	$\delta^{13}\text{C}_{\text{PDB}}$	Rock
<i>Amphibolite facies (Ussuri)</i>		
02-1	–8.5	Granite gneiss
02-4	–8.7	Plagiogneiss
03-1	–8.6	Biotite granite gneiss
03-1a	–8.7	Graphite vein
03-3	–8.6	Garnet–biotite–graphite schist
03-5	–8.5	Lamprophyre
<i>Greenschist facies (Mitrofanovka)</i>		
04-22	–19.9	Sericite–quartz–graphite shale
04-24	–19.3	Sericite–quartz–graphite shale
04-17	–25.2	Sericite–graphite–quartz shale
04-34	–23.7	Sericite–quartz–graphite shale
04-40	–26.6	Quartz–sericite–graphite shale

800 spectrometer at the Laboratory of Diamond Mineralogy, Institute of Geology, Ural Branch of Russian Academy of Sciences (Syktyvkar, Russia).

4. Results

4.1. Graphite mineralogy and geochemistry

In all the varieties of rocks present in the study area, a high degree of graphitization, including graphitic metasomatism, is ideal for studying the graphite. Graphite occurs as monomineralic veins and lenticular inclusions in the igneous protholiths and skarns, and it is also widespread as dispersed lamellae, ranging in size from 200 nm to 2 mm, that are oriented along the foliation of the gneisses and schists. The relationships with other minerals in thin section indicate that it crystallized at the same time as the other metamorphic minerals, forming mutual intergrowths with biotite, sericite, chlorite, and quartz, or as inclusions in feldspar and pyroxene. This suggests that the regional carbonization coincided in time with the regional metamorphism.

As a mineral with a constant composition, graphite varies in texture and morphology according to the P–T conditions of formation. Graphites in veinlets in rocks metamorphosed under the amphibolite facies have textural parameters that correspond to the high-crystalline variety (Table 6). Individual graphite flakes from the samples listed in Table 5 were analyzed, including sample

03-1a, a graphite vein in granite gneiss; 03-3, a garnet–biotite feldspar schist; and 03-5, a lamprophyre. The points for individual flake measurements were chosen under reflected light. The studied samples are obviously inhomogeneous, and contain three optically discernible varieties of carbonaceous matter: flaky graphite that is bright in reflected light and with crystallites that exceed 100 nm in size (Table 7), fine-grained flaky graphite that forms xenomorphic aggregates (Table 8), and micrometric (1–3 μm) inclusions of amorphous carbonaceous matter within flaky graphite. Some of the inclusions have weak luminescence (Fig. 2a), but others are bluish with relative strong luminescence (Fig. 2b). Apart from the wide D and G bands, the inclusions provide spectra with rather distinct bands at 1086–1088 and 1197–1235 cm^{-1} , and a mathematically defined wide band of 1475–1484 cm^{-1} (Table 9). The spectra of the three varieties are shown in Fig. 3.

The isotopic compositions of the carbon in rocks metamorphosed under the amphibolite and greenschist facies also illustrate the inhomogeneity of the carbonaceous matter (Table 4). Graphite in the core of the Ruzhino metamorphic dome has stable carbon isotopic compositions with $\delta^{13}\text{C} = -8.7 \pm 0.1\text{‰}$, inherent in all rocks of the amphibolite facies. According to Faure (1986), values of $\delta^{13}\text{C}$ close to -7‰ characterize an endogenous crustal source of carbon. The carbon isotopic compositions in greenschist-facies graphite–sericite–quartz schists have lower $\delta^{13}\text{C}$ values that range from -19.3‰ to -26.6‰ , which is typical of organic carbon in marine sediments (Naidu et al., 1993).

4.2. Noble metal mineralization

The forms of the noble metal–graphite mineralization were studied mainly with SEM and a Zeiss Libra-120 transmission electron microscope (TEM) with a HADDF detector and δ -filter. The TEM method involves electron energy-loss spectroscopy, providing an EELS image, which represents the qualitative distribution of elements with high sensitivity. It also allowed us to detect the characteristic losses of the $\text{O}_{2,3}$ and $\text{M}_{4,5}$ energy of platinum (Fig. 4a and b), which is an indicator of Pt in graphite.

SEM analyses show that thin-prismatic crystals of isoferroplatinum (Pt = 90.36 wt%, Fe = 9.64 wt%) exist in the graphite–sericite–quartz schist of the Mitrofanovka Formation (Fig. 5). Subprismatic microcrystals (up to 2–3 μm) containing platinum and an admixture of other elements (Pt = 79.31 wt%, C = 8.65 wt%, Cu = 2.09 wt%, Si = 1.05 wt%, and O = 8.93 wt%) were also found in graphite-bearing metasomatic rocks in the Tamga and Turgenevo deposits. The noted admixture of C, O, and Si may be spurious and a consequence of the minute dimensions of the platinum crystals being set in a silicate–carbonaceous matrix.

Inclusions of globular gold in the graphite-bearing rocks are common, and an example of a spheroidal aggregate of gold with inclusions of thin graphite flakes is shown in Fig. 6. The SEM analyses revealed significant compositional variations in this gold grain with Au = 100.0–79.3 at.%, Ag = 0.0–22.02 at.%, and Cu = 0.0–2.2 at.%. The flakes of graphite enclosed in the gold also have heterogeneous compositions according to the measurements at three points (C = 57.92–71.25 at.%, Au = 0.46–17.4 at.%, O = 28.2–30.3 at.%, Cl = 0.25–2.06 at.%, K = 0.0–2.05 at.%, Ca, Si, and Al = 0.0–1.7 at.%). A carbonaceous nanofilm (100–200 nm thick), revealed by SEM on the gold spheroid, contains an admixture of Cl, S, Ca, Al, and Fe up to 1–2 wt% in addition to the carbon (56–60 wt%) and oxygen (19–33 wt%). It is another example of the co-precipitation of gold and carbonaceous matter from an ore-bearing metamorphic fluid. Native gold in the skarns differs from that in the graphite-bearing rocks, and is characterized by its crystal form, compositions with higher contents of silver (up to 10 wt%), and larger-sized spongy and lamellar crystals (Fig. 7). Gold in the quartz veins contains admixtures of W (1.26 wt%), F

Table 6
Results of X-ray phase analyses of graphite from rocks of the Ussuri Formation.

hkl	Database ICDD, nm	03-1a		03-3		03-5		04-64		Error Δd , nm
		d, nm	I, rel %							
002	0.336	0.335	100	0.335	100	0.335	100	0.335	100	0.006
100	0.213		1	0.213	1			0.212	1	0.0018
101	0.203	0.202	1	0.202	1	0.203	1			0.0016
102	0.180					0.1788	1	0.1798	1	0.001
004	0.1678	0.1676	6	0.1677	5	0.166	5	0.1676	5	0.001
103	0.1544	0.1537	1	0.1540	1	0.1538	1	0.1537	1	0.0008
110	0.1232	0.1228	1			0.1230	1			0.0004
112	0.1158	0.1152	1			0.1151	1			0.0003
006	0.1120	0.1118	1	0.1118	1	0.1118	1	0.1118	1	0.0001
114	0.0990					0.0989	1			
008	0.0840	0.0838	1	0.0838	1	0.0838	1	0.0838	1	0.0001
Parameters of the elementary cell, nm										
a	0.2465	0.2449 ± 0.0005		0.2450 ± 0.0007		0.2452 ± 0.0005		0.2455 ± 0.0005		
c	0.6721	0.6702 ± 0.0009		0.6706 ± 0.0014		0.6701 ± 0.0010		0.6699 ± 0.0009		
V	0.3537	0.3482 ± 0.0014		0.349 ± 0.002		0.3490 ± 0.0015		0.3496 ± 0.0015		

Table 7
Raman spectroscopy data for flaky graphite in the Turgenevo and Tamga deposits.

No sample/spectrum	Position of bands, cm^{-1}		1	2	3
	D	G			
04-64/1	1356	1581	16	0.04	>100
04-64/6	–	1581	14	0	>100
04-64/7	1353	1582	19	0.13	10–100
03-1a/1	1352	1582	14	0.17	>100
03-1a/4	1360	1581	15	0.36	>100
03-1a/7	1353	1580	17	0.19	10–100
03-5/1	1355	1581	15	0.24	>100
03-5/7	–	1581	14	0	>100
03-3/4	1353	1580	14	0.07	>100
03-3/6	1353	1580	17	0.21	10–100
03-3/7	1352	1581	15	0.15	>100
03-3/8	1350	1581	15	0.18	>100
Сре.мее	1354	1582	15	–	>100

Note: 1 = width of the G band at the half-height, cm^{-1} ; 2 = proportions of band intensities I_D/I_G , exciting radiation $\perp(002)$; 3 = crystalline size L_a , nm.

(up to 34.66 wt%), and U (3.42 wt%), and these admixtures, including the fluorine, increase in amount from the centers of the grains outwards. The grain margins of the gold are coated with a fragmentary carbonaceous nanofilm ranging from 100 to 200 nm thick (Table 10).

Along with platinum and gold, graphite-bearing rocks of the Khanka terrane contain many inclusions of native copper, zinc, nickel, bismuth, Ir–REE, Fe–Cr, Cu–Sn, Cu–Sn–Fe intermetallics, Ag minerals (AgI, AgCl, AgBr, Ag(Cl, Br, I), and Hg_3Ag_2), oxides (such as Fe_3O_4 , SnO_2 , and YPO_4), monazite, and other REE minerals

Table 8
Raman spectroscopy data for fine-grained graphite in the Turgenevo and Tamga deposits.

Sample #/spectrum	Position of the bands, cm^{-1}		1	2	2	Remark
	D	G				
04-64/3	1350	1581	16	0.10	44	Luminescence
04-64/4	1353	1581	18	0.14	31	
03-1a/2	1355	1579	16	0.23	19	
03-1a/3	1352	1575	20	0.30	15	
03-5/2	1354	1580	17	0.25	18	Luminescence
03-5/9	1347	1570	25	0.55	8	
03-3/5	1353	1580	59	0.32	14	
03-3/9	1348	1577	18	0.27	16	
03-3/10	1351	1580	19	0.64	7	
middle	1351	1578	23	0.27	19	

Note: Note: 1 = width of the G band at the half-height, cm^{-1} ; 2 = proportions of band intensities I_D/I_G , exciting radiation $\perp(002)$; 3 = crystalline size L_a , nm.

(Khanchuk et al., 2010, 2013). Sulfides, such as pyrite, arsenopyrite, galena, and argentite, occur only as accessory, exotic minerals. This is an essential difference between the studied rocks and deposits of the black shale type that normally contain appreciable amounts of sulfides (Laverov et al., 2000; Distler et al., 2004).

4.3. Noble metal contents in the studied rock complex

The quantitative determinations of gold and PGE, reported in Tables 3 and 4, show that the contents of Au and PGE are elevated in all lithological varieties of the graphite-bearing metamorphic rocks. These data were further supported by AAS-TEA analyses of Pt, Pd, Au, and Ag in graphite-bearing lamprophyre, schist, granite gneiss, skarn, mica–quartz shale, phyllite-like shale, and a diabase dike (Table 11). The AAS-TEA method proved to be the most accurate, as the samples with extremely high Pt contents reveal the presence of multiple nanometric grains of platinum under the electronic microscope. The noble metal contents in the rocks vary significantly, so that Pt concentrations range from 0.33 to 62.63 ppm, with the highest amounts found in lamprophyres and the diabase dikes. Au concentrations range from 0.001 to 4.75 ppm, Ag contents from 0.17 to 4.41 ppm, and Pd from 0.01 to 3.85 ppm. These data reflect the irregular distribution of noble metals in the rocks studied.

About 40 samples from the Khanka terrane were first analyzed by the oxidative fluoridation method. Analytical results for 12 of these samples are presented in Table 3, with contents (ppm) ranging as follows: Au (0.02–6.73), Ag (0.2–4.41), Pt (0.014–0.116), Pd (0.02–0.55), Ir (0.002–0.055), Os (0.011–0.09), Ru (0.007–0.2),

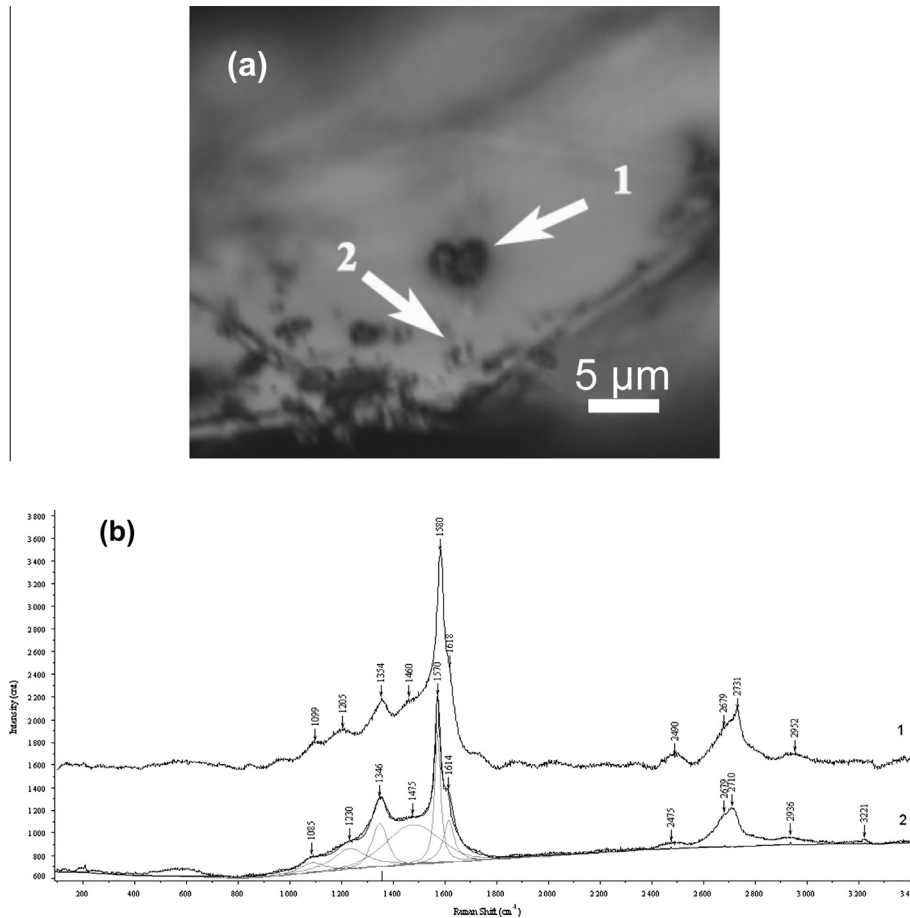


Fig. 2. (a) SEM-image of diamond-like luminescent carbon included in a graphite flake. (b) Raman spectra corresponding to points (1) and (2) on (a).

Table 9

Raman spectroscopy data for amorphous carbon in the Turgenevo and Tamga deposits.

No sample/spectrum	Position of bands cm^{-1}		1	2	3	4
	D	G				
03-5/6	1346	1571	27	0.30	1088 (113) 1235 (152) 1475 (245)	A
03-5/8	1342	1576	47	0.24	1086 (100) 1197 (135) 1484 (189)	B

Note: 1 = width of the G band at the half-height, cm^{-1} ; 2 = proportion of band intensities I_D/I_G ; 3 = additional bands (width at the half-height), cm^{-1} ; 4 = diamond-like carbon. Luminescence: A = weak, B = strong.

and Rh (0.001–0.74). The results of the noble metal analyses using this method show that all Rh and most of the Au, Pt, and Pd passed into solution during the process of a single fluorine oxidation, whereas Ru, Os, and Ir, which were analyzed after repeated dissolutions, were completely retained in the insoluble graphitic residue of the first dissolution. The results of the stepwise decomposition of graphite-bearing samples confirm the incorporation of some of the noble metals into graphite, which suggests that the noble metals and the graphite were formed contemporaneously.

5. Discussion

The current analytical results, as well as the data we obtained by X-ray and Raman spectroscopy, provide grounds for concluding that there are at least two generations of graphite in the graphite-

bearing rocks we have studied. The first generation is represented by nanocrystalline graphite with relatively low temperatures of exothermal maxima (860–900 °C), and the second by crystallites that are larger than 100 nm in size and which have relatively high temperatures of exothermal maxima (950–1000 °C), according to the thermogravimetric data (Plyusnina et al., 2013a,b). In contrast to the second generation of graphite, which has regular Raman spectra, the early graphite exhibits several hydrocarbon bonds, and has the appearance of separate carbonaceous material in the form of bitumen that is responsible for the luminescence at the surface of the nanocrystalline graphite (Fig. 2). The formation of primary bitumen takes place by endogenic carbonization under the influence of metalliferous and reduced carbon-bearing fluids. The circulation of these fluids in a highly permeable rock complex would be accompanied by the crystallization of graphite if the temperature and pressure rapidly decreased, leading to oversaturation

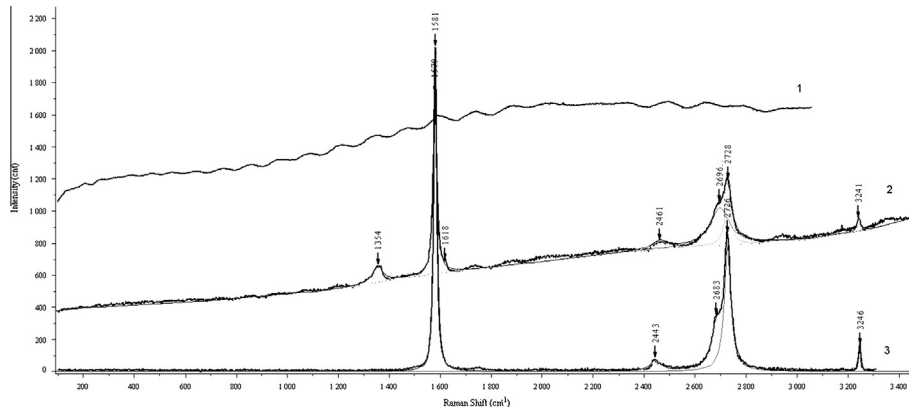


Fig. 3. Raman spectra of varieties of carbonaceous matter in lamprophyre sample 03-5: 1, bitumoid; 2, nanocrystalline graphite; 3, highly-ordered flaky graphite.

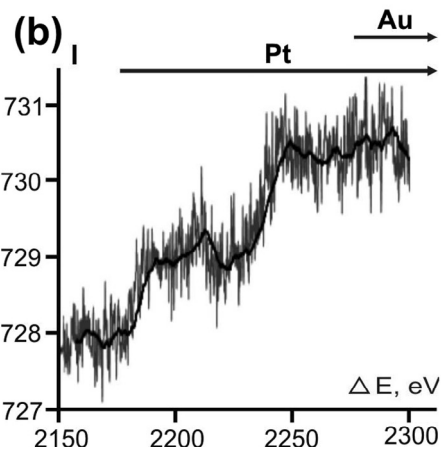
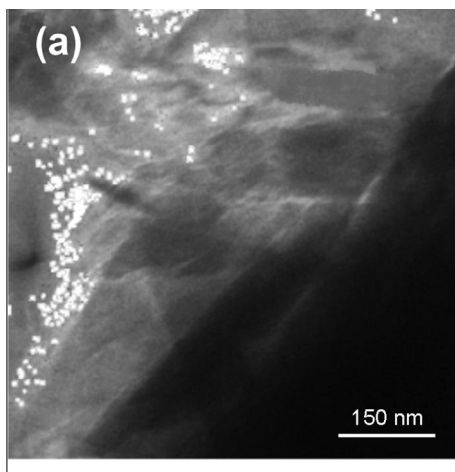


Fig. 4. (a) EELS image of graphite flake including an assemblage of dispersed nano-sized crystals of natural platinum. (b) Spectrum of characteristic losses of $M_{4,5}$.

of carbon in the fluids (Salotti et al., 1971; Connolly, 1995). This concept is supported by the usual occurrence of graphite-bearing rocks in the permeable zones of disjunctive structures, from microstructures to large-scale normal faults and thrusts. Graphite of the second generation was formed by recrystallization of carbon-bearing terrigenous rocks during a regional metamorphism.

Discrimination of the two graphite varieties on the basis of their physical parameters is consistent with the data obtained from their chemical decomposition (Table 2). AAS analyses demonstrate that the noble metals are mostly associated with graphite. Micro-flakes

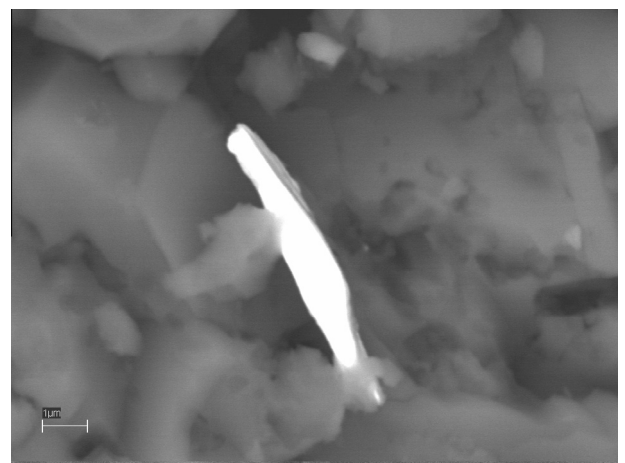


Fig. 5. SEM image of a thin prismatic microcrystal of isoferroplatinum set in a matrix of graphite and silicate material.

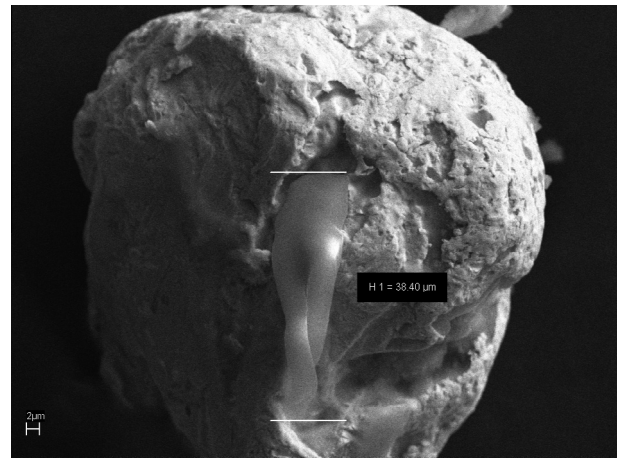


Fig. 6. SEM image of the micro-spheroid form of gold that here contains a graphite flake inclusion.

of graphite pass into solution during the first decomposition by hydrofluoric acid, while the large-flakes are more resistant to decomposition. The second-generation graphite concentrates all the silver, ruthenium, osmium, and iridium, while graphite of the first generation concentrates the gold, rhodium, and platinum (Table 3). The association of the second-generation graphite with

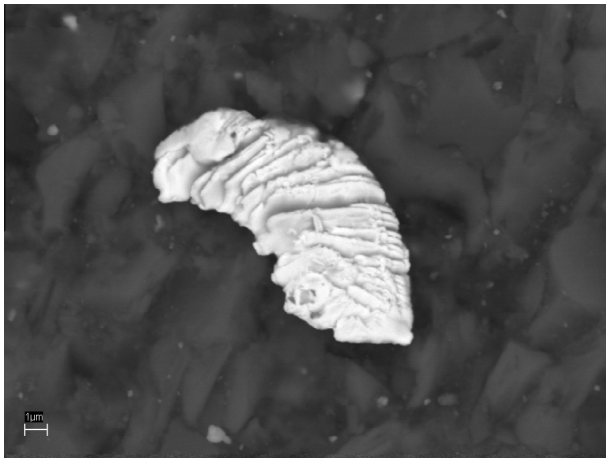


Fig. 7. SEM image of gold lamellar crystals in the silicate-carbonaceous matrix of a graphite-sericite-quartz shale.

Table 10
Gold grain and carbonaceous film compositions (wt%) from SEM analyses of Tamga graphite (Fig. 1).

Element	Gold grain			Film
	1	2	3	
C	–	8.47	20.98	19.83
O	–	11.21	13.56	65.69
F	2.17	10.41	34.66	–
Mg	–	1.01	5.68	0.55
Na	–	–	–	0.36
Al	–	1.2	7.98	3.94
Si	–	–	1.06	7.24
Cl	–	–	–	0.13
K	–	–	1.53	0.71
Ca	–	–	–	0.3
Fe	–	–	0.53	1.25
Cu	–	1.94	1.0	–
Ag	30.85	20.88	3.58	–
Au	63.56	42.26	9.44	–
U	3.42	1.36	–	–
W	–	1.26	–	–
Total	100	100	100	100

Note: 1 → 3 – from center to rim of a gold grain.

Table 11
Noble metal contents (ppm) in graphitic rocks of the Khanka terrane.

Sample	Pt	Pd	Au	Ag	Rock
AP-1(1)	57.28	1.30	2.08	3.37	Lamprophyre
AP-1(2)	16.86	1.29	0.28	1.35	
AP-1(3)	0.70	0.14	1.33	1.03	Crystalline schist
AP-15	0.33	0.01	1.90	0.70	Granite
AP-15/4A	2.14	–	0.07	0.17	Skarn
AP-15/11	1.83	0.31	0.15	0.34	
AP-18/1	0.41	0.12	0.41	0.85	Biotite-feldspar schist
AP-22/3	4.02	0.06	0.06	0.56	Muscovite-biotite schist
AP-22/4	6.31	0.30	2.19	1.57	
AP-24	16.05	0.51	0.15	0.65	Biotite-graphite-sericite schist
AP-35/5	6.93	0.04	4.75	0.48	Graphite-sericite-quartz shale
AP-36/2	62.63	0.98	0.11	4.41	Diabase
AP-36/2a	56.88	3.85	0.41	2.93	
AP-36/4	3.29	0.18	0.05	0.50	Phyllite
AP-38/8	1.40	1.19	0.001	0.63	Phyllite
AP-40/4	1.62	1.00	0.06	3.80	

Note: analyses were performed using AAS TEA, and the samples were chemically decomposed by a mixture of concentrated acids.

metamorphic recrystallization is illustrated by the presence of graphite veins in biotite, and of biotite inclusions in graphite. Thus, the graphitization in the Tamga and Turgenevo deposits, as well as the associated noble-metal mineralization, was a result of polychronous and polygenetic processes.

The measured O and H isotopic compositions ($D_{\text{vs}mow} = -82.5\text{‰}$ to 106.7‰ and $^{18}\text{O}_{\text{vs}mow} = 8.2\text{‰}$ to 10.1‰) of biotite associated with graphite from the Ruzhino amphibolite-facies rocks (Khanchuk et al., 2013) are close to the isotopic compositions that are typical of both magmatic waters and the mantle (Mattey, 1987; Deloule et al., 1991), and they are also close to those of magmatic biotites in the Bushveld mafic-ultramafic complex (Harris and Chaumba, 2001). The contribution of the mantle to the mineralization in the Khanka amphibolite-facies rocks is manifested by the isotopic composition of carbon (Table 5), and also by the relationship $\text{Pt} > \text{Au}$, which is an indicator of a mantle origin. On the other hand, when the concentrations are the other way round ($\text{Au} > \text{Pt}$), it is typical of hydrothermal alteration in the crust and black-shales (Distler et al., 2004). The Au and PGE mineralization hosted by metasedimentary rocks of the Mitrofanovka Formation may have been precipitated from a heterogeneous oxidized hydrothermal fluid, which had been affected by the organic matter of the host rocks (Table 5). Thus, both the deep reduced fluids and the terrigenous rocks can be sources of carbon in such rock complexes. According to experimental data, carbonaceous matter has a high sorption capacity that increases with temperature, so that the sorption capacity of graphite measured at 500 °C is 2700 ppm for gold and about 1000 ppm for platinum in monometallic systems (Plyusnina et al., 2004). These values exceed the sorption capacity of amorphous carbonaceous matter at 200 and 300 °C , due to the emission of hydrogen and its replacement by metals in aromatic rings when heating up to 500 °C (Bel'skii et al., 1997). The existence of organoplatinum complexes as protophases for metallic platinum crystallization has been indicated by an experimental study of the Pt-C-S-H₂O system (Plyusnina et al., 2013a,b). Moreover, quantum-chemical modeling has shown a strong energy of interaction exists between graphene fragments and clusters of Pt(0) (Medkov et al., 2010). In addition, the highest interaction energy was detected for horizontal platinum clusters located between graphite sheets, indicating that they can form so-called graphite intercalation compounds (Dunaev et al., 2008). These results explain the well-known difficulties of detecting any visible platinum phases in graphite-bearing rocks with a microscope, even if the platinum content is high, as measured by physiochemical analysis (Khanchuk et al., 2010).

It is valid to assume that gold and platinum can be transported as carbonyl, halogen-carbonyl, and other carbon-bearing complexes that are stable at temperatures of up to $400\text{--}500\text{ °C}$. Complex organoplatinum compounds, described in sublimates of gaseous fluids at the Kudryavy volcano (Kuril Islands), correspond to $\text{PtCl}_2[\text{P}(\text{C}_4\text{H}_9)_3]_2$ (Distler et al., 2008). Analogs of Se and Re were also found there along with Pt complexes. Further cooling under oxidative conditions will destabilize the complex compounds, releasing native metals, intermetallides, and carbonates. Furthermore, destruction of these compounds will release volatile components and metallic clusters with the subsequent aggregation and enlargement of metallic clusters. Experiments have shown that carbonaceous matter has a higher buffer capacity in relation to redox-potential than do hematite-magnetite and pyrite-pyrrhotite-magnetite assemblages (Plyusnina et al., 2000). This is a result of the transformation of carbonaceous matter on heating with the release of a number of gas constituents such as CH_4 , CO , CO_2 , and H_2 . The redox regime of metamorphic rocks in the Ussuri Formation is determined by the endogenic graphitization reaction $\text{CH}_4 + \text{O}_2 = \text{C} + \text{H}_2\text{O}$, which is the principal redox-controlling reaction in systems at temperatures below 500 °C . Another devolatilization

Table 12
Trace element contents (ppm) of rocks from the Ussury and Mitrofanovka formations.

Sample	02/1	02/3	03/3	04/8	04/17	04/40	04/85	04/101
Be	1.28	3.57	0.99	2.23	1.78	2.26	0.66	6.30
Sc	2.00	2.4	30.7	28.5	11.7	22.6	1.00	12.8
V	14.70	4.20	170.8	196.9	132.0	351.9	9.39	91.03
Cr	7.65	6.85	102.2	136.3	36.25	78.34	25.90	430.1
Co	0.81	2.25	22.77	13.90	2.59	0.89	1.45	8.98
Ni	3.85	7.16	39.67	73.68	9.88	4.15	8.97	37.51
Cu	3.62	16.60	5.74	12.61	23.47	58.89	28.64	20.99
Zn	20.6	36.3	235.0	124.4	6.00	4.9	2.3	238.1
Ga	9.97	16.45	26.79	31.19	11.59	20.51	1.77	29.18
Rb	286.9	287.7	240.1	284.3	70.47	119.1	5.01	448.6
Sr	249.3	130.2	240.3	520.0	51.74	44.23	3520	303.3
Y	3.04	22.88	44.29	25.66	38.52	79.57	5.80	49.59
Zr	49.2	49.03	229.5	246.8	91.6	207.6	3.75	205.2
Nb	1.79	3.24	12.85	15.95	9.41	20.31	0.56	20.33
Mo	0.14	0.29	0.36	0.35	5.99	39.40	0.29	0.55
Cd	0.05	0.06	0.33	0.25	0.12	0.24	0.14	0.35
Sn	1.10	2.56	2.52	3.22	0.87	2.35	1.74	5.31
Cs	5.38	8.41	5.04	7.68	1.97	3.59	0.12	19.69
Ba	1276	313	942.4	814.0	3733	5534	69.00	940.0
La	22.40	22.81	41.80	47.08	19.02	54.87	4.95	47.81
Ce	42.02	45.15	92.63	101.5	27.71	86.83	9.33	105.2
Pr	4.63	5.70	11.15	12.17	3.73	13.65	1.17	12.26
Nd	16.15	20.18	45.60	48.64	12.15	53.78	4.43	45.05
Sm	2.87	4.92	9.00	8.65	2.54	12.17	1.06	10.48
Eu	1.49	0.79	1.99	1.46	0.61	2.47	0.54	1.27
Gd	2.07	4.68	9.24	6.78	4.42	12.79	0.84	10.51
Tb	0.17	0.80	1.27	0.90	0.80	1.93	0.13	1.62
Dy	0.57	4.49	9.22	5.21	5.83	12.06	0.75	9.81
Ho	0.12	0.89	1.80	1.08	1.33	2.78	0.18	1.69
Er	0.20	2.18	4.73	3.16	4.05	7.98	0.51	4.41
Tm	0.03	0.33	0.69	0.52	0.57	1.23	0.08	0.64
Yb	0.19	2.12	5.00	3.96	3.79	8.33	0.47	3.84
Lu	0.03	0.29	0.77	0.59	0.54	1.22	0.07	0.53
Hf	1.34	1.95	6.75	7.25	2.54	5.43	0.09	6.17
Ta	0.20	0.95	0.81	0.94	0.62	1.24	0.04	2.15
W	0.87	5.28	0.53	1.40	0.95	2.20	2.20	4.69
Pb	48.45	66.32	34.38	27.12	17.48	10.96	6.37	93.57
Th	8.39	25.80	12.96	14.16	8.36	12.07	0.77	39.47
U	0.57	8.09	2.92	2.29	7.72	8.71	0.48	13.80

Note: samples 02/1 and 02/3 are granite-gneisses; 03/3 is schist; 04/8 is amphibolite; 04/17 and 04/40 are graphite-sericite-quartz shales; 04/85 is skarn; 04/101 is lamprophyre. ICP-MS analyses were performed at the Analytical Center of the Far East Geological Institute, Russian Academy of Sciences, Vladivostok, Russia.

equilibrium $\text{CO}_2 + \text{CH}_4 = 2\text{C} + 2\text{H}_2\text{O}$ (Ohmoto and Kerrick, 1977) may allow graphite to form at a higher temperature. Widespread biotite-graphite intergrowths suggest that the formation of most graphite was most likely to have been controlled by a reaction leading to graphite precipitation in close association with hydrous silicates.

A wide range of REE and trace element contents, determined with ICP-MS using an Agilent 7500 spectrometer, are listed in Table 12, and they clearly demonstrate the origin of geochemically different components that were inherited from both felsic and mafic rocks. Analyses of a variety of graphite-bearing rocks indicate that they all contain elements such as Zr, Sr, Ga, La, Ba, Rb, Ni, Ti, V, Cr, and Cu, and we interpret the elevated concentrations of Ti, V, Cr, Ni, and Cu as typical of rock complexes in intraplate zones, where fluids transport elements scavenged from the lower crust and upper mantle (Cartigny et al., 2001; Dacheng et al., 2004). The effect of deep-seated basic magma chambers is seen in the injection of lamprophyre dikes of gabbro-diorite composition, and which have high contents of REEs, phosphates, and PGE. The studied graphite-ore complex displays the following features typical of noble metal deposits in zones of mantle-crustal diapirism: the spatial restriction of horst-anticlinal structures, the significant vertical amplitude of the graphite mineralization, the occurrence of granitoids of various compositions, lamprophyre dikes, elevated concentrations of noble metals, and a close association of the noble metals with graphite. These features are peculiar

to ore deposits that can be described as magmatic-fluid types (Vinokurov et al., 1997; Craw, 2002; Crespo et al., 2006).

6. Conclusions

Elevated noble metal concentrations within the study area suggest the preference of these metals for graphite-bearing metamorphic rocks. The highest concentrations of noble metals in the Khanka terrane are confined to highly permeable zones that contain widespread dislocations, and it seems that such heterogeneous terranes are both chemically and structurally favorable to fluid circulation. Based on the data summarized above, it can be assumed that graphite has been transported and deposited by C–O–H–halogen-bearing fluids of magmatic origin, and this idea is most applicable to the metamorphic rocks of the Ussuri group. The other alternative form of transportation involves the crystallization of graphite during the regional metamorphism of carbon-bearing sedimentary rocks, and this idea seems most applicable to the greenschist-facies rocks of the Mitrofanovka Formation.

Dispersed micro- and nano-sized segregations of gold and platinum-group elements, and their inhomogeneous admixtures with carbon, halogens, and oxygen, provide evidence for noble metals crystallizing from carbon-bearing gaseous fluids.

The behavior of gold and platinum in the metamorphic rocks of the Ussuri and Mitrofanovka formations indicates polygenetic and

polychronous processes of neomineralization, in conjunction with multiple graphitization events, regional metamorphism, and the formation of skarns. In total, three sources of noble-metal mineralization can be distinguished: (1) an endogenic magmatic fluid related to mantle–crustal magma chambers, (2) an exogenic sedimentary–chemogenetic source related to the formation of the graphite–sericite–quartz shales of the Mitrofanovka Formation, and (3) a metamorphic source related to the transfer of metals during regional metamorphism.

Acknowledgments

The Russian Foundation for Basic Research (Project 11-05-00848) and the Chinese Foundation for Natural Sciences (Project 14-05-91159) supported this study financially, and that support is greatly appreciated by the authors. We are also grateful to Dr. G.G. Sikhharulidze, Dr. V.N. Mitkin, and G.A. Scheka for physico-chemical analyses; to Dr. N.N. Barinov and Dr. P.P. Safonov for SEM images, EDA analyses, and Raman spectroscopy; and to Dr. S.I. Isaenko, G.A. Modyanova, and B.A. Makeev from the Institute of Geology, Komi Scientific Center, Ural Branch, Russian Academy of Sciences, for XRD and thermogravimetric analyses.

References

- Ballhaus, J.J., Stampfl, E.F., 1985. Occurrence and petrological significance of graphite in the upper Critical Zone, western Bushveld complex, South Africa. *Earth Planet. Sci. Lett.* 74, 58–68.
- Bel'skii, N.K., Nebolsina, L.A., Oksenoid, I.G., 1997. Decomposition of samples in the determination of platinum-group metals in carbonaceous rocks. *Zh. analiticheskoy khim.* 52 (1), 132–135 (In Russian).
- Boudreau, A.E., McCallum, I.S., 1992. Concentration of platinum-group elements by magmatic fluids in layered intrusions. *Econ. Geol.* 87, 1830–1848.
- Cartigny, P., Jendrzewski, N., Pineau, F., Petit, E., Javoy, M., 2001. Volatile (C, N, Ar) variability in MORB and the respective roles of mantle source heterogeneity and degassing: the case of the southwest Indian Ridge. *Earth Planet. Sci. Lett.* 194, 241–257.
- Chamberlain, J.A., 1967. Sulfides in the Muskox intrusion. *Can. J. Earth Sci.* 4, 105–153.
- Connolly, J., 1995. Phase diagram methods for graphitic rocks and application to the system C–O–H–FeO–TiO₂–SiO₂. *Contrib. Mineral. Petrol.* 119, 94–116.
- Craw, D., 2002. Geochemistry of late metamorphic hydrothermal alteration and graphitisation of host rock, Macraes Gold mine, Otago schist, New Zealand. *Chem. Geol.* 191, 257–275.
- Crespo, E., Luque, F.J., Rodas, M., Wada, H., Gervilla, F., 2006. Graphite–sulfide deposits in Ronda and Beni Bousera peridotites (Spain and Morocco) and the origin of carbon in mantle-derived rocks. *Gondwana Res.* 9, 279–290.
- Dacheng, J., Ruizhong, H., Yan, L., Xuelin, Q., 2004. Collision belt between the Khanka block and the North China block in the Yanbian region, Northeast China. *J. Asian Earth Sci.* 23, 211–219.
- Deloule, V.V., Albaredo, F., Sheppard, S.M.F., 1991. Hydrogen isotope heterogeneities in the mantle from ion probe analysis of amphiboles from ultramafic rocks. *Earth Planet. Sci. Lett.* 105, 543–553.
- Distler, V.V., Yudovskaya, M.A., Mitrofanov, C.I., Prokofev, V.Y., Lishnevskii, E.N., 2004. Geology, composition, and genesis of the Sukhoi Log noble metals, Russia. *Ore Geol. Rev.* 24, 7–44.
- Distler, V.V., Dikov, Y.P., Yudovskaya, M.A., 2008. Platinum–chlorine–phosphorus–hydrocarbon complex in volcanic fluids: the first find in the terrestrial environment. *Dokl. Earth Sci.* 420, 628–631.
- Dunaev, A.V., Arkhangelskii, I.V., Zubavichus, Y.A., Avdeev, V.V., 2008. Preparation, structure and reduction of graphite intercalation compounds with hexachloroplatinic acid. *Carbon* 46, 788–795.
- Faure, G., 1986. *Principles of Isotope Geology*, second ed. Wiley.
- Ferry, J.M., 1996. Prograde and retrograde fluid flow during contact metamorphism of siliceous carbonate rocks from the Ballachulish aureole, Scotland. *Contrib. Mineral. Petrol.* 124, 235–254.
- Galvez, M.E., Beyssac, O., Martinez, J., Benzerara, K., Chaduteau, C., Malvoisin, B., Malavielle, J., 2013. Graphite formation by carbonate reduction during subduction. *Nat. Geosci.* 6, 473–477.
- Harris, C., Chaumba, J.B., 2001. Crustal contamination and fluid–rock interaction during the formation of the Platreef, northern limb of the Bushveld complex, South Africa. *J. Petrol.* 42, 1321–1347.
- Khanchuk, A.I., Plyusnina, L.P., Molchanov, V.P., 2004. The first data on gold–platinoid mineralization in carbonaceous rocks of the Khanka massif and prediction of a large noble metals deposit in Primorye. *Dokl. Earth Sci.* 397, 820–824.
- Khanchuk, A.I., Plyusnina, L.P., Molchanov, V.P., Medvedev, E.I., 2010. Carbonization and geochemical characteristics of graphite-bearing rocks in the northern Khanka terrane, Primorye, Russian Far East. *Geochem. Int.* 48, 107–111.
- Khanchuk, A.I., Nechaev, V.P., Plyusnina, L.P., Berdnikov, N.V., Molchanov, V.P., Vysotskii, S.V., 2013. Noble-metal–graphite mineralization: a comparative study of the carbonaceous granite–gneiss complex and shales of the Russian Far East. *Ore Geol. Rev.* 53, 276–286.
- Korzinskii, D.S., 1965. The theory of systems with perfectly mobile components and process of mineral formation. *Am. J. Sci.* 263, 193–205.
- Kucha, H., 1981. Precious metal alloys and organic matter in the Zechstein copper deposits, Poland. *Mineral. Petrol.* 28, 1–16.
- Laverov, N.P., Prokofev, V.Y., Distler, V.V., 2000. New data on conditions of ore deposition and composition of ore-forming fluids in the Sukhoi Log gold–platinum deposit. *Dokl. Earth Sci.* 371, 357–361.
- Leapman, R.D., Newbury, D.E., 1993. Trace element analysis at nanometer spatial resolution by parallel-detection electron energy-loss spectroscopy. *Anal. Chem.* 65, 2409–2414.
- Manning, C.E., 2004. The chemistry of subduction-zone fluids. *Earth Planet. Sci. Lett.* 223, 1–16.
- Mattey, D., 1987. Carbon isotopes in the mantle. *Terra Cognita* 7, 31–38.
- Medkov, M.A., Khanchuk, A.I., Voit, A.V., Plyusnina, L.P., Molchanov, V.P., Medvedev, E.I., 2010. Quant chemical study of the interaction between Au (0), Pt(0), Ag(0) and fragments of graphenes modelling graphite structure. *Dokl. Earth Sci.* 434, 1321–1324.
- Melcher, F., Crum, W., Simon, C., Thalhammer, T.V., Stumpfl, E., 1997. Petrogenesis of ophiolitic giant chromite deposit of Kempirsai, Kazakhstan. *J. Petrol.* 38, 1419–1458.
- Mitkin, V.N., Galizky, A.A., Korda, T.M., 2000. Some observations on the determination of gold and the platinum-group elements in black shales. *Geostandards Newsletter* 24, 227–240.
- Mitkin, V.N., Khanchuk, A.I., Likhoidov, G.G., Zayakina, S.B., Galizky, A.A., Tzimbali, V.G., 2009. Study of reference sample candidate for the noble metal contents (PGM, Au, Ag) in graphitized rocks. *Dokl. Earth Sci.* 424, 133–138.
- Mogessie, A., Stumpfl, E.F., Weiblen, P.W., 1991. The role of fluids in the formation of platinum group minerals, Duluth complex, Minnesota: mineralogical, textural and chemical evidence. *Econ. Geol.* 86, 1506–1518.
- Naidu, A.S., Scalani, R.S., Feder, N.M., 1993. Stable organic carbon isotopes in sediments of the North Bering–South Chukchi seas, Alaskan–Soviet Arctic shelf. *Cont. Shelf Res.* 13, 669–691.
- Ohmoto, H., Kerrick, D., 1977. Devolatilization equilibria in graphitic systems. *Am. J. Sci.* 277, 1013–1044.
- Ortega, L., Millward, D., Luque, F.J., Barrenechea, J.F., Beyssac, O., Huizenga, J.M., Rodas, M., Clarke, S.M., 2010. The graphite deposit at Borrowdale (UK): a catastrophic mineralizing event associated with Ordovician magmatism. *Geochim. Cosmochim. Acta* 74, 2429–2449.
- Plyusnina, L.P., Kuz'mina, T.V., Likhoidov, G.G., Narnov, G.A., 2000. Experimental modeling of platinum sorption on organic matter. *Appl. Geochem.* 15, 777–784.
- Plyusnina, L.P., Kuz'mina, T.V., Avchenko, O.V., 2004. Modeling of gold sorption on carbonaceous matter at 20–500 °C and 1 kbar. *Geochem. Int.* 42, 755–763.
- Plyusnina, L.P., Khanchuk, A.I., Kuz'mina, T.V., Barinov, N.N., Likhoidov, G.G., 2013a. Sorption extraction of crystalline platinum from aqueous solutions to a carbon film. *Dokl. Chem.* 453, 273–275.
- Plyusnina, L.P., Schumilova, T.G., Isaenko, S.I., Likhoidov, G.G., Ruslan, A.V., 2013b. Graphite of the Turgenevskoe and Tamginskoe deposits of the Lesozavodsk area in the Primor'e region. *Russ. J. Pacific Geol.* 7 (4), 288–298.
- Rumble III, D., Duke, F., Hoering, T.L., 1986. Hydrothermal graphite in New Hampshire: evidence of carbon mobility during regional metamorphism. *Geology* 14, 452–455.
- Salotti, C.A., Heinrich, E.W., Gairdini, A.A., 1971. Abiotic carbon and the formation of graphite deposits. *Econ. Geol.* 66 (6), 929–932.
- Sikharulidze, G.G., 2004. Ionic source with a hollow cathode for element analysis of solids. *Mass-Spectrometriya* 1 (1), 21–30 (in Russian).
- Sikharulidze, G.G., 2009. Modernization of the element 2 mass spectrometer. *Instrum. Exper. Tech.* 52 (2), 242–244.
- Vinokurov, S.F., Novikov, Yu.N., Usatov, A.V., 1997. Fullerenes in the geochemistry of endogenic processes. *Geochem. Int.* 35, 822–828.
- Volborth, A.J., Housley, R.M., 1984. A preliminary description of complex graphite, sulfide, arsenide, and platinum group elements mineralization in a pegmatoid pyroxenite of the Stillwater complex, Montana, USA. *Mineral. Petrol.* 33, 213–230.
- Wright, A.J., Parnell, J., Ames, D.E., 2010. Carbon spherules in Ni–Cu–PGE sulfide deposits in the Sudbury impact structure, Canada. *Precamb. Res.* 177, 23–38.
- Yermolaev, N.P., 1995. Platinum-group metals in terrigenous carbonaceous shales. *Geochem. Int.* 32, 122–132.